Dynamic polarization potential induced by the Coulomb excitation of deformed heavy ions: Geometric scattering approach

N. Takigawa
Department of Physics, Tohoku University, 980 Sendai, Japan

F. Michel
Faculté des Sciences, Université de Mons-Hainaut, B-7000 Mons, Belgium

A. B. Balantekin
Physics Department, University of Wisconsin, Madison, Wisconsin 53706

G. Reidemeister
Faculté des Sciences, Université Libre de Bruxelles, B-1050 Bruxelles, Belgium
(Received 3 December 1990)

The geometric scattering theory and the Wentzel-Kramers-Brillouin (WKB) approximation are used to derive explicit expressions for the dynamic polarization potential induced by Coulomb excitation in heavy-ion collisions involving strongly deformed targets. We build two phase-equivalent potentials with very different radial and angular-momentum behaviors, which are discussed in the context of polarization potentials obtained previously within different frameworks. This correspondence provides a recipe for approximately correcting the deficiencies of the geometric scattering approach, which tends to overemphasize the effects of Coulomb coupling.

I. INTRODUCTION

In the study of heavy-ion collisions, the contribution of the large number of channels at high excitation energy, which are only weakly coupled to the entrance channel, can generally be incorporated in a conventional optical model, the parameters of which are expected to vary smoothly and systematically with incident energy and mass number. One of the basic questions is to identify and estimate the components of the optical potential arising from specific inelastic modes strongly coupled to the entrance channel, the so-called dynamic polarization potential (DPP).[1,2] These contributions can significantly differ from one system to another since they reflect the idiosyncrasies of the nuclei under study. A well-known example is provided by the long-range absorption due to Coulomb excitation, which is known to have a dramatic impact on the elastic cross section when the target displays strong deformation. A textbook example[1-3] is the case of the $^{18}O+^{184}W$ system at 90 MeV, studied experimentally by Thorn *et al.*,[4] which displays an elastic-scattering angular distribution differing considerably from the standard Fresnel pattern. By performing explicit coupled-channel calculations, Thorn *et al.*[4] were able to show that the deviation from the Fresnel pattern is mainly caused by Coulomb excitation of the ^{184}W nucleus to its first $I^{\pi}=2^{+}$ rotational excited state (Fig. 1). Subsequently, Love, Terasawa, and Satchler[5] (LTS) built the DPP corresponding to this coupling; this was found to be mainly imaginary, to have a very long range (it behaves essentially as $1/r^5$), and to be l independent. In another study, Baltz, Kauffmann, Glendenning, and Pruess[6] (BKGP) presented another version of the DPP, with seemingly quite different properties (strong angular-momentum dependence, r dependence expressed as a combination of r^{-3}, r^{-4}, and r^{-5} dependences), but giving an equivalent description of the experimental data. Despite its very different properties, this potential was shown to be comparable to the LTS potential near the classical turning point for each partial wave. Fröbrich, Lipperheide, and Fiedeldey[7] (FLF) confirmed these two calculations by explicitly constructing the DPP by an inversion procedure starting from the results of Coulomb excitation calculations; their DPP, which is l-independent, was found to be very similar to the LTS potential, and also to the l independent equivalent of the BKGP potential.

In the present paper, we derive explicit expressions of the DPP in a novel way, starting from a geometric scattering approach to strong-coupling effects in heavy-ion reactions. This approach,[8] which is based on the introduction of the no-Coriolis and the adiabatic approximations, makes it possible to completely decouple the initial coupled-channel equations into a set of ordinary Schrödinger equations, where the bare potential is supplemented with a term proportional to the coupling form factor. It provides a completely different physical picture of the departure of the experimental cross section from the standard Fresnel pattern.[9] Although the main results of a complete coupled-channel calculation can be reproduced qualitatively in this simple approach, the model is found to overemphasize the effects of Coulomb excitation, but it was pointed out by several authors[10,11] that reducing the strength of the Coulomb coupling Hamil-

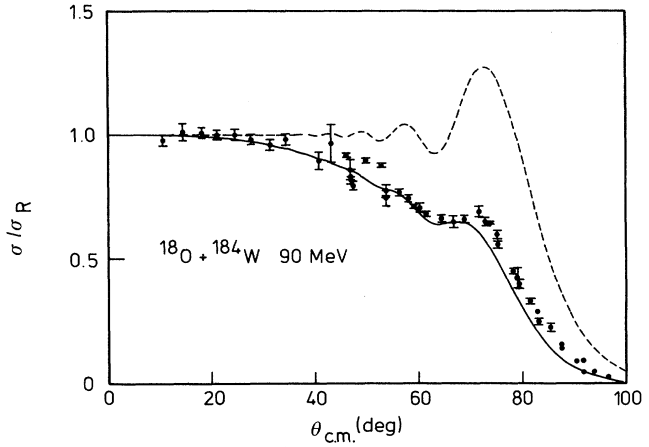

FIG. 1. Comparison of the experimental elastic-scattering angular distribution of Thorn *et al.* (Ref. 4) for $^{18}O+^{184}W$ at 90 MeV, with coupled-channel calculations using the parameters of Ref. 5 and taking only Coulomb coupling into account (solid line). The dashed line is the prediction of the bare potential.

tonian by about 20% makes a quantitative reproduction of the exact calculation possible. This puzzling result, as well as the coexistence of two phase-equivalent DPP's with very different properties, naturally emerge from the present study.

Our paper is organized as follows. In Sec. II, we briefly sketch the geometric scattering theory, emphasizing its implications for the description of elastic scattering. Section III is devoted to the derivation of general expressions of the DPP in terms of the coupling form factor, starting from the geometric scattering theory and from the Wentzel-Kramers-Brillouin (WKB) approximation to the S matrix. In Sec. IV, these results are applied to the case of long-range Coulomb coupling; we show explicitly how our approach generates DPP's in semiquantitative agreement with those of Refs. 5 and 6, shedding light on the link between these very different potentials. The renormalization of the deformation parameter needed to bring the geometric scattering approach in quantitative agreement with exact calculations is also discussed. Section V presents a summary of our paper.

II. THE ELASTIC-SCATTERING S MATRIX IN THE GEOMETRIC SCATTERING THEORY

In the case of the excitation of members of a $K^\pi=0^+$ ground-state rotational band of an axially symmetric deformed nucleus, the coupled-channel equations read,[1,2] in standard notations

$$\left[-\frac{\hbar^2}{2\mu}\frac{d^2}{dr^2}+\frac{\hbar^2}{2\mu r^2}l_1(l_1+1)+U(r)-E_{I_1}\right]f_{I_1,l_1}(r)$$
$$+F_\lambda(r)\sum_{I_2,l_2}(-)^{J+l_2}i^{I_2+l_2-I_1-l_1}\left[\frac{(2l_1+1)(2I_1+1)(2I_2+1)}{2\lambda+1}\right]^{1/2}$$
$$\times\langle I_1 I_2 00|\lambda 0\rangle\langle l_1\lambda 00|l_2 0\rangle\begin{Bmatrix} l_1 & I_1 & J \\ I_2 & l_2 & \lambda\end{Bmatrix}f_{I_2,l_2}(r)=0\ , \quad (1)$$

where I and l denote the angular momenta for the rotational state excited and for the relative motion, respectively. The optical potential $U(r)$ contains an imaginary part in order to take into account the effects on the scattering of the other intrinsic degrees of freedom. The multipolarity λ of the intrinsic excitation is two if we restrict to quadrupole deformation. In general, the coupling form factor $F_2(r)$ consists of Coulomb and nuclear parts:

$$F_2(r)=F_2^{(C)}(r)+F_2^{(N)}(r)\ , \quad (2)$$

where

$$F_2^{(C)}(r)=\sqrt{5/4\pi}\,\tfrac{3}{5}\beta_2^{(C)}Z_1Z_2e^2\left[\frac{R_C^{(T)}}{R_C}\right]^2 f_C(r)\ , \quad (3)$$

with

$$f_C(r)=\begin{cases}\dfrac{R_C^2}{r^3} & \text{for } r\geq R_C\ ,\\ \dfrac{r^2}{R_C^3} & \text{for } r<R_C\ ,\end{cases} \quad (4)$$

and

$$F_2^{(N)}(r)=-\sqrt{5/4\pi}\beta_2^{(N)}R_N^{(T)}\frac{d}{dr}U_N(r)\ . \quad (5)$$

In Eqs. (3)–(5), β_2 is the deformation parameter, and the superscripts (C), (N), and (T) stand for the Coulomb and nuclear parts, and the target, respectively.

The geometric scattering theory makes use of two approximations.[8,9] The first is the no-Coriolis approximation, where the change in the centrifugal potential due to the finite multipolarity of the intrinsic excitation is neglected, which amounts to replacing $l_1(l_1+1)$ in Eq.

(1) by $J(J+1)$, where J denotes the total angular momentum in the entrance channel. The second is the adiabatic approximation, where the finite excitation energy of the rotational motion is ignored [E_{I_1} in Eq. (1) is replaced by the c.m. energy E in the entrance channel]. Subjecting Eq. (1) to the unitary transformation which diagonalizes the coupling matrix, one obtains a set of decoupled equations which read

$$\left[-\frac{\hbar^2}{2\mu}\frac{d^2}{dr^2}+\frac{\hbar^2}{2\mu r^2}J(J+1)+U(r)+\lambda_\alpha F_2(r)-E\right]\phi_\alpha(r)=0\ , \quad (6)$$

where the λ_α denote the eigenvalues of the coupling matrix, and where the wave functions $\phi_\alpha(r)$ in the "pseudochannels" are related to the physical wave functions by the unitary transformation which performs this diagonalization. If the description of the rotational band is truncated at $I=I_{\max}$, the number of decoupled Schrödinger equations (6) to be solved to calculate the physical S matrix is given by $\alpha_{\max}=I_{\max}/2+1$.[8] For example, if we restrict the possible excitation to the $I^\pi=2^+$ member of the rotational band, the number of equations to be solved reduces to $\alpha_{\max}=2$ (whereas there were four coupled equations in the physical channels). The eigenvalues λ_α which determine the strength of the correction to the diagonal potential in each pseudochannel are given by[8]

$$\lambda_\alpha=P_2(\cos\theta_\alpha)\ , \quad (7)$$

where $\cos\theta_\alpha$ are the zeros of $P_{I_{\max}+2}$ with $\theta_\alpha<\pi/2$. The physical S matrix in the elastic channel is given in terms of the S matrix in each pseudochannel, $S^{(\alpha)}$, by[8]

$$S=\sum_{\alpha=1}^{\alpha_{\max}} w_\alpha S^{(\alpha)}\ , \quad (8)$$

where the w_α are the weight factors used in the $(I_{\max}+2)$-point Gauss-Legendre quadrature formula[12] (in fact, only half of these is needed by symmetry). Equation (8) is obtained by using the boundary conditions for the scattering problem and the properties of the unitary matrix which connects the physical and the pseudochannel wave functions. Equation (8) underlies the interpretation of the geometric scattering approach:[8] the scattering process can be viewed in terms of the superposition of a few elementary scatterings, corresponding to fixed orientations of the deformed target with respect to the beam direction. The relevant orientations are determined by the maximum I value at which the truncation of the rotational band is made; notice, however, that these orientations only determine the strength of the potential to be used in each pseudochannel and do not correspond to anisotropic potentials.

III. DERIVATION OF TWO ALTERNATIVE DPP's FROM THE GEOMETRIC SCATTERING THEORY

We will derive two possible explicit expressions for the DPP starting from the geometric scattering theory and the WKB expression of the phase shift. In this last approximation, the elastic S matrix is given by[13]

$$S_l=\exp\left[2i\int_{r_{0l}}^{\infty}\left[\frac{2\mu}{\hbar^2}[E-V_l(r)]\right]^{1/2}dr\right]\ , \quad (9)$$

where $V_l(r)$ denotes the effective potential for angular momentum l,

$$V_l(r)=U(r)+\frac{\hbar^2}{2\mu}\frac{l(l+1)}{r^2}\ , \quad (10)$$

and r_{0l} is the distance of closest approach for this wave. Here and in the following the angular-momentum index l will consistently be dropped, as well as the multipolarity index $\lambda=2$. The potential renormalization $\lambda_\alpha F(r)$ used in pseudochannel α will thus induce a modification of the bare S matrix, S_0, given up to second order in λ_α by

$$S_0\to S^{(\alpha)}=S_0\exp\left[-i\left[\frac{2\mu}{\hbar^2}\right]^{1/2}\lambda_\alpha\int_{r_0}^{\infty}\frac{F(r)}{\sqrt{E-V(r)}}dr\right]\times\exp\left[-\frac{1}{4}i\left[\frac{2\mu}{\hbar^2}\right]^{1/2}\lambda_\alpha^2\int_{r_0}^{\infty}G(r)dr\right]\ , \quad (11)$$

where we have introduced

$$G(r)=\frac{[F(r)-\kappa_0V'(r)]^2}{[E-V(r)]^{3/2}}+2\kappa_0\frac{\kappa_0V''(r)-2F'(r)}{[E-V(r)]^{1/2}}\ , \quad (11')$$

$$\kappa_0=\frac{F(r_0)}{V'(r_0)}\ ; \quad (11'')$$

in this expression, account has been taken of the shift of the turning point due to the perturbation. A sketch of the derivation of Eqs. (11) can be found in the Appendix.

Use of Eq. (8) for the elastic-scattering S matrix, together with the following identities for the eigenvalues λ_α and weight factors w_α:[8,9]

$$\sum_{\alpha=1}^{\alpha_{\max}} w_\alpha=1,\quad \sum_{\alpha=1}^{\alpha_{\max}} w_\alpha\lambda_\alpha=0,\quad \sum_{\alpha=1}^{\alpha_{\max}} w_\alpha\lambda_\alpha^2=\tfrac{1}{5}\ , \quad (12)$$

leads to the following expression for the elastic-scattering S matrix:

$$S=S_0\exp\left[\frac{-\mu}{5\hbar^2}\left[\int_{r_0}^{\infty}\frac{F(r)}{\sqrt{E-V(r)}}dr\right]^2\right]\times\exp\left[-\frac{1}{20}i\left[\frac{2\mu}{\hbar^2}\right]^{1/2}\int_{r_0}^{\infty}G(r)dr\right]\ , \quad (13)$$

valid up to second order in the deformation parameter. Note that the pseudochannel S matrix $S^{(\alpha)}$ differs from the bare S matrix by terms of *first* order in the deformation parameter β_2; in Eq. (13), terms linear in β_2 are absent because of the second identity of Eq. (12). It is also seen that expression (13) of the S matrix has become independent of $\alpha_{\max}$. Dependence on $\alpha_{\max}$ would be recovered if the expansions used in deriving (13) were carried out to higher order in λ_α. In that case the identities of Eq. (12) would have to be supplemented with simi-

lar expressions corresponding to higher powers n in λ_α, which turn out to depend on $\alpha_{\max}$ for $n>3$ (this can be proved easily by applying the $2\alpha_{\max}$-point Gauss-Legendre quadrature formula to the integral of $[P_2(\cos\theta)]^n$ over $\cos\theta$).

As a modification $U(r)\to U(r)+\delta V(r)$ of the bare potential induces to lowest order in δV the modification

$$S_0\to S_0\exp\left[-i\left[\frac{2\mu}{\hbar^2}\right]^{1/2}\int_{r_0}^{\infty}\frac{\delta V(r)}{\sqrt{E-V(r)}}dr\right] \tag{14}$$

of the bare S matrix, the modification of Eq. (13) predicted by the geometric scattering theory is equivalent to the introduction of a DPP satisfying

$$\int_{r_0}^{\infty}\frac{\delta V(r)}{\sqrt{E-V(r)}}dr=-i\frac{1}{10}\left[\frac{2\mu}{\hbar^2}\right]^{1/2}\times\left[\int_{r_0}^{\infty}\frac{F(r)}{\sqrt{E-V(r)}}dr\right]^2+\frac{1}{20}\int_{r_0}^{\infty}G(r)dr\ . \tag{15}$$

Since this constraint appears through an integral condition, several expressions for the DPP are consistent with Eq. (15). The most trivial one is

$$\delta V_a(r)=\frac{1}{20}G(r)[E-V(r)]^{1/2}-i\frac{1}{10}\left[\frac{2\mu}{\hbar^2}\right]^{1/2}F(r)\int_{r_0}^{\infty}\frac{F(r_1)}{\sqrt{E-V(r_1)}}dr_1\ ; \tag{16}$$

another obvious alternative is

$$\delta V_b(r)=\frac{1}{20}G(r)[E-V(r)]^{1/2}-i\frac{1}{5}\left[\frac{2\mu}{\hbar^2}\right]^{1/2}F(r)\int_{r}^{\infty}\frac{F(r_1)}{\sqrt{E-V(r_1)}}dr_1\ . \tag{17}$$

These two phase-equivalent DPP's are seen to have very different r-dependences; this point will be discussed more fully in the next section.

IV. APPLICATION TO LONG-RANGE COULOMB COUPLING

We will apply Eqs. (16) and (17) to the case where long-range Coulomb coupling dominates the scattering. This is, e.g., the case for the system under investigation, that is, $^{18}O+^{184}W$ at 90 MeV, where taking Coulomb coupling into account made it possible[4] to obtain a very satisfactory description of the spectacular departure of the elastic-scattering cross section from the Fresnel pattern, which we discussed in the Introduction. Furthermore, here we will restrict to high partial waves, where the distance of closest approach is larger than the range of the nuclear forces.

In this case $V(r)$, $\rho_0=kr_0$, and $F(r)$ reduce to

$$V(r)=E\left[\frac{2\eta}{\rho}+\frac{L^2}{\rho^2}\right], \tag{18}$$

$$\rho_0=(L^2+\eta^2)^{1/2}+\eta\ , \tag{19}$$

$$F(r)=\sqrt{5/4\pi}\tfrac{3}{5}\beta_2^{(C)}Z_1Z_2e^2\frac{(R_C^{(T)})^2}{r^3}\ , \tag{20}$$

where we have introduced the Langer replacement $L=l+\frac{1}{2}$, the Sommerfeld parameter η, and the reduced variable $\rho=kr$.

The integral appearing in Eqs. (16) and (17) can be evaluated explicitly; one obtains, for $r\geq r_0$,

$$\int_r^{\infty}\frac{1/r_1^3}{\sqrt{E-V(r_1)}}dr_1=\frac{k^2}{\sqrt{E}L^2}\left\{\left[1-\left[1-\frac{2\eta}{\rho}-\frac{L^2}{\rho^2}\right]^{1/2}\right]-\frac{\eta}{L}\left[\sin^{-1}\frac{L^2/\rho+\eta}{(L^2+\eta^2)^{1/2}}-\sin^{-1}\frac{\eta}{(L^2+\eta^2)^{1/2}}\right]\right\}. \tag{21}$$

For large values of L, this becomes independent of L up to third order in $1/\rho$, and reduces to

$$\int_r^{\infty}\frac{1/r_1^3}{\sqrt{E-V(r_1)}}dr_1\simeq\frac{k^2}{2\sqrt{E}}\frac{1}{\rho^2}\left[1+\frac{2\eta}{3\rho}\right]. \tag{22}$$

A. Comparison with the LTS long-range absorptive potential

Equation (17) leads to the following expression of the DPP in the case of pure Coulomb excitation:

$$\delta V_b(r)=\tfrac{1}{20}G(r)[E-V(r)]^{1/2}-i\frac{1}{5}\frac{A^2k^3}{EL^2}\frac{1}{r^3}\left\{1-\left[1-\frac{2\eta}{kr}-\left[\frac{L}{kr}\right]^2\right]^{1/2}-\frac{\eta}{L}\left[\sin^{-1}\frac{L^2/kr+\eta}{(L^2+\eta^2)^{1/2}}-\sin^{-1}\frac{\eta}{(L^2+\eta^2)^{1/2}}\right]\right\}; \tag{23}$$

to leading order in $1/r$ the imaginary part of the DPP behaves as

$$\mathrm{Im}\delta V_b(r) \simeq \frac{1}{5}\left[\frac{2\mu}{\hbar^2}\right]^{1/2}\frac{A^2}{2\sqrt{E}}\frac{1}{r^5} . \tag{23'}$$

In Eqs. (23) and (23'), the constant A stands for

$$A = \sqrt{4\pi/5}Z_1 e\sqrt{B_T(E2)\uparrow} , \tag{24}$$

where we have used the well-known relation between the deformation parameter and the $B(E2)$ value.[2]

To lowest order in $1/r$, the imaginary part of δV_b has the same $1/r^5$ dependence as the long-range absorptive DPP of Ref. 5. Also, the weak, $E^{-1/2}$ energy dependence of δV_b is the same as that of the LTS polarization potential. In fact, to lowest order in $1/r$, one has

$$\frac{\mathrm{Im}\delta V_b}{\mathrm{Im}\delta V_{\mathrm{LTS}}} = \frac{3}{2} . \tag{25}$$

If we compare δV_b and δV_{LTS} to next order in $1/r$, this result still holds to a good approximation. Indeed, one has to this order,

$$\delta V_b(r) \propto \frac{1}{\rho^5}\left[1+\frac{2\eta}{3\rho}\right] . \tag{26}$$

On the other hand, the $1/r^5$ dependence of the DPP of LTS must be corrected for taking into account the braking of the particles in the presence of the Coulomb field; in the so-called local-energy approximation, and beyond the range of nuclear forces, the r^{-5} dependence of the LTS potential becomes[5]

$$\delta V_{\mathrm{LTS}} \propto \frac{1}{\rho^5}\left[1-\frac{2\eta}{\rho}\right]^{-1/2} \simeq \frac{1}{\rho^5}\left[1+\frac{\eta}{\rho}\right] . \tag{27}$$

Although the corrective terms in Eqs. (26) and (27) differ by a factor of 1.5, they have the same energy and radial behaviors and comparable magnitudes. The result of Eq. (25) can thus be considered to still provide a reasonable estimate. To check the accuracy of the various approximations used, we compare in Fig. 2 the exact DPP obtained from Eq. (21) for several l values with the approximate expression obtained from Eq. (26), and with the LTS polarization potential. It can be seen that the l dependence of our exact DPP is indeed weak, and that the result of Eq. (25) holds to a good approximation.

The absolute value of the real part of the DPP turns out to be much smaller than that of the imaginary part. This can be seen in Fig. 2 where we have plotted the real part of Eq. (23) for $l=0$ and 60. The real part of the DPP can thus be neglected, as was also found to be the case for the LTS (Ref. 5) and BKGP (Ref. 6) polarization potentials.

Equation (25) indicates that the results of exact coupled-channel calculations can be reproduced with good accuracy within the geometric scattering approach by reducing the strength of the coupling Hamiltonian. Indeed, Eq. (25) implies that renormalizing $\beta_2^{(C)}$ by a factor of about $(\frac{2}{3})^{1/2}=0.82$ should bring our DPP in better agreement with that of LTS, and therefore an approximate compensation for the effects of the no-Coriolis approximation in geometric scattering calculations should be obtained by use of this recipe. A comparable factor was obtained empirically by Esbensen *et al.*[10] in a study of ^{58}Ni+^{162}Dy at 345 MeV. In the closely related formalism of the angle-dependent phase shifts, Lipperheide *et al.*[11] had similarly to renormalize the Coulomb radius parameter of the target from $r_{0C}^{(T)}=1.25$ to 1.10 fm to get quantitative agreement with the exact results in their study of the ^{12}C+Nd and ^{16}O+Sm systems around 70 MeV. As, in the outside region, the strength of the coupling Hamiltonian is determined by the product $\beta(R_C^{(T)})^2$, this amounts to renormalizing the Coulomb deformation parameter by a factor $(1.10/1.25)^2=0.77$, which is close to the factor 0.82 quoted above.

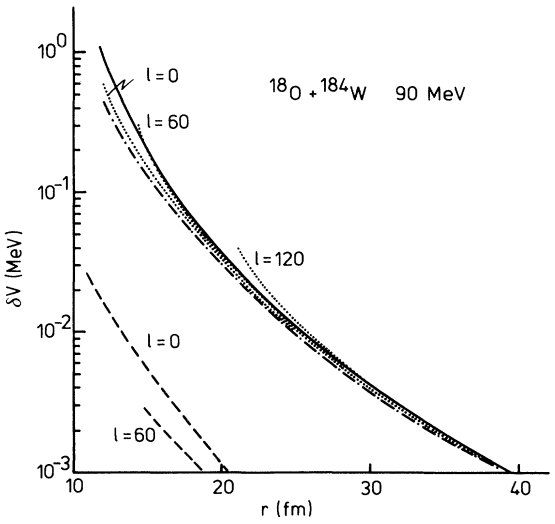

FIG. 2. Comparison of the imaginary part of the exact dynamic polarization potential δV_b of Eq. (23) (dotted lines) and its approximate l-independent version of Eq. (26) (dash-dotted line), with the LTS potential[5] (solid line) for the ^{18}O+^{184}W system at 90 MeV. The dashed lines represent the real part of δV_b. The δV_b curves have been multiplied by $\frac{2}{3}$ (see text).

In Fig. 3, we show the effect of reducing $\beta_2^{(C)}$ from its physical value $\beta_2^{(C)}=0.236$ (used with $R_C^{(T)}=6.84$ fm) to

$$\beta_2^{(C)}=0.236\times 0.82=0.194$$

in the geometric scattering calculation of ^{18}O+^{184}W at 90 MeV. This figure shows that the large deviation from the Fresnel pattern is qualitatively well accounted for by the model using the original deformation parameter, but that renormalizing the strength of the coupling as explained above reproduces the results of the exact coupled-channel calculations in a quantitative way.

To conclude this section, let us stress that the simple recipe of renormalizing the strength of the coupling by $\sqrt{2/3}$ is expected to hold only in the case of pure Coulomb coupling, and provided the corrective terms appearing in Eqs. (26) and (27) are small in the region of physical interest. Also, we have omitted in the above discussion the adiabaticity correction factor $g_2(\xi)$ of Ref. 5, which for heavy-ion systems involving strong

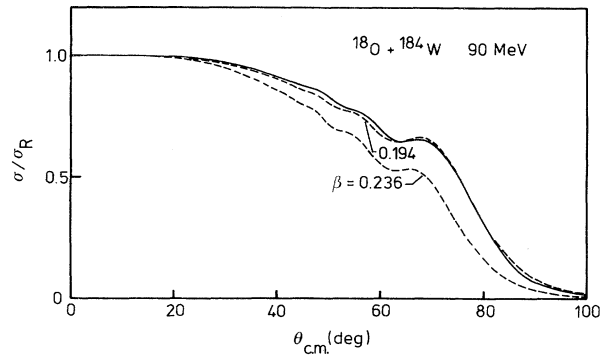

FIG. 3. Comparison of exact coupled-channel calculations for $^{18}O+^{184}W$ at 90 MeV (solid line), with the geometric scattering approach predictions (dashed lines) obtained using (a) the physical value of the deformation parameter $\beta_2^{(C)}=0.236$, and (b) the renormalized value $\beta_2^{(C)}=0.194$.

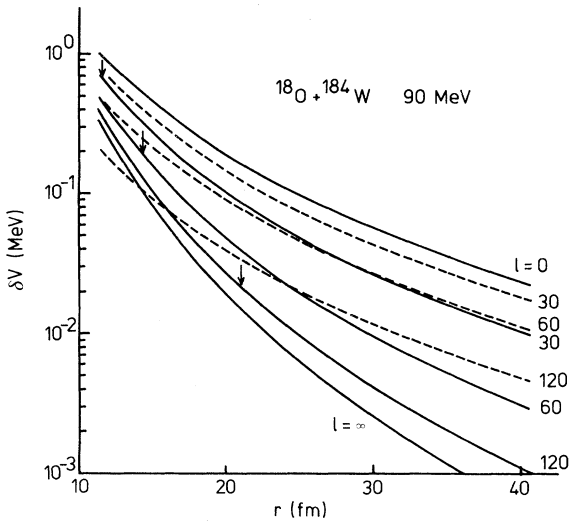

FIG. 4. Comparison of the exact dynamic polarization potential δV_a of Eq. (28) (dashed lines) with the BKGP potential (Ref. 6) (solid lines) for the $^{18}O+^{184}W$ system at 90 MeV. The arrows indicate the classical turning points for the displayed l values.

deformations—and thus small excitation energies—is very close to unity.[5]

It should also be emphasized that our conclusions are restricted to the case where multiple excitation is not important, since our DPP does not depend on the number α_{max} of states of the rotational band included. It has been shown by FLF (Ref. 7), that, in cases where multiple Coulomb excitation is important, as in the $^{40}Ar+^{238}U$ system, the imaginary part of the DPP is significantly lower than the predictions of both the LTS and BKGP approaches, which are restricted to single-excitation processes; whether our renormalization recipe retains some validity in these more complicated cases is an open question.

B. Comparison with the BKGP polarization potential

The alternative choice of Eq. (16) leads to a DPP with very different r and l dependences. Indeed, the imaginary part of $\delta V_a(r)$ now behaves like $1/r^3$ instead of $1/r^5$, and instead of being nearly l independent, $\delta V_a(r)$ has a strong l dependence through the lower bound of the integral, which is nothing but the classical turning point for angular momentum l. One finds explicitly, using Eqs. (16), (19), and (21),

$$\mathrm{Im}\delta V_a(r) = -\frac{1}{10}\left[\frac{2\mu}{\hbar^2}\right]^{1/2}\frac{A^2}{r^3}\frac{k^2}{\sqrt{E}L^2}\left[1-\frac{\eta}{L}\tan^{-1}\frac{L}{\eta}\right]. \quad (28)$$

Although this DPP is not identical with the BKGP polarization potential,[6] one can prove the following connections:

(i) For $l\to 0$, both potentials are identical (in particular, they both behave like $1/r^3$).

(ii) Both potentials decrease monotonically when l increases; the BKGP potential tends to a fixed $1/r^5$ behavior when $l\to\infty$, whereas our potential behaves like $1/r^3$ whatever l, and tends to zero when $l\to\infty$. However, our potential remains twice as large as the BKGP potential at the classical turning point when l tends to infinity.

Our polarization potential $\delta V_a(r)$ is compared, for the $^{18}O+^{184}W$ system at 90 MeV, with the BKGP potential for several l values in Fig. 4. As in the work of BKGP, the arrows denote the location of the turning points for the l values illustrated.

Although the DPP of Eq. (28) is not identical to the BKGP potential, our calculation sheds light on the coexistence of phase-equivalent potentials with very different properties. The phase equivalence of the LTS and BKGP potentials has been proven by FLF (Ref. 7) by a direct construction of the l-independent equivalent of the BKGP potential, which turns out to be nearly identical to the LTS potential.

V. SUMMARY

In this paper, we have combined the geometric scattering theory and the WKB approximation to discuss the properties of the dynamic polarization potential (DPP) in the case of the scattering of heavy ions from a strongly deformed target, where the long-range Coulomb excitation dominates, and where multiple excitation processes do not dominate the scattering.

Phase equivalence with the geometric scattering approach, which imposes a constraint on the DPP through the integral condition (15), can be satisfied by several expressions; Eqs. (16) and (17) are obvious choices for satisfying this constraint. We have shown that one of these choices leads to a nearly purely imaginary DPP, showing a $1/r^5$ behavior, with very weak l-dependence, nearly identical to the polarization potential of Love, Terasawa, and Satchler[5] up to a factor of $\frac{3}{2}$. In contrast, the second choice leads to a strongly l dependent, $1/r^3$ potential, whose connections with the polarization potential of

Baltz, Kauffmann, Glendenning, and Pruess[6] have been emphasized.

As a by-product, we have obtained a prescription for correcting the deficiencies of the no-Coriolis approximation, which underlies the geometric scattering approach, and which tends to overemphasize the effects of Coulomb excitation: a better quantitative agreement with exact coupled-channel calculations can be obtained by reducing the deformation parameter by a factor of $\sqrt{\frac{3}{2}}$.

ACKNOWLEDGMENTS

One of us (N.T.) thanks Professor R. Ceuleneer and Dr. C. Semay for their kind hospitality while he stayed in Mons, where this work was completed. This research project was supported in part by the exchange program between Japan and Belgium by the Japan Society for the Promotion of Science, in part by the University of Wisconsin Research Committee with funds granted by the Wisconsin Alumni Research Foundation, and in part by the U.S. National Science Foundation. N.T. also thanks Professor K. W. McVoy and Professor W. Friedman for their kind hospitality while he visited Madison, where part of this work has been done. F.M. and G.R. are grateful to Professor R. Ceuleneer for his support during the course of this work.

APPENDIX: DERIVATION OF EQS. (11)

The modification of the nuclear phase shift induced by the change $\Delta V(r)=\lambda_a F(r)$ of the potential reads, in the WKB approximation,

$$\Delta\delta=\lim_{R\to\infty}\left[\int_{r_0+\Delta r_0}^{R}\left[\frac{2\mu}{\hbar^2}(E-V-\Delta V)\right]^{1/2}dr-\int_{r_0}^{R}\left[\frac{2\mu}{\hbar^2}(E-V)\right]^{1/2}dr\right]. \tag{A1}$$

Each of these integrals tends to infinity with R, but the difference of Eq. (A1) tends to a well-defined finite limit when R goes to infinity. Δr_0 denotes the shift of turning point induced by the potential change.

Writing these integrals in dimensionless form, by introducing the reduced quantities $\mathcal{V}(\rho)=V(r)/E$, $\rho=kr$, etc., and rearranging the first integral, we can rewrite Eq. (A1) as

$$\Delta\delta=\lim_{R\to\infty}\left[\int_{\rho_0}^{R}\sqrt{1-\mathcal{V}(\rho+\Delta\rho_0)-\Delta\mathcal{V}(\rho+\Delta\rho_0)}\,d\rho-\int_{\rho_0}^{R}\sqrt{1-\mathcal{V}(\rho)}\,d\rho\right]-\Delta\rho_0 . \tag{A1'}$$

To second order in the perturbation, the shift of the turning point is given by

$$\Delta\rho_0=\frac{\Delta\mathcal{V}_0}{\mathcal{V}_0'}+\frac{\Delta\mathcal{V}_0\Delta\mathcal{V}_0'}{\mathcal{V}_0'^2}-\frac{1}{2}\frac{\Delta\mathcal{V}_0^2\mathcal{V}_0''}{\mathcal{V}_0'^3}, \tag{A2}$$

where $\mathcal{V}_0\equiv\mathcal{V}(\rho_0)$, etc.; to the same order, the difference between the integrands of Eq. (A1') reads

$$\sqrt{1-\mathcal{V}(\rho+\Delta\rho_0)-\Delta\mathcal{V}(\rho+\Delta\rho_0)}-\sqrt{1-\mathcal{V}(\rho)}=-\frac{1}{2(1-\mathcal{V})^{1/2}}[\Delta\rho_0\mathcal{V}'+\Delta\mathcal{V}+\tfrac{1}{2}(\Delta\rho_0)^2\mathcal{V}''+\Delta\rho_0\Delta\mathcal{V}']-\frac{1}{8(1-\mathcal{V})^{3/2}}(\Delta\rho_0\mathcal{V}'+\Delta\mathcal{V})^2 . \tag{A3}$$

It is easily seen using Eqs. (A1'), (A2), and (A3) that the modification of the phase shift is given, to first order in the perturbation, by

$$\Delta\delta^{(1)}=-\tfrac{1}{2}\int_{\rho_0}^{\infty}\frac{\Delta\mathcal{V}(\rho)}{\sqrt{1-\mathcal{V}(\rho)}}d\rho , \tag{A4}$$

which gives the first exponential in Eq. (11).

The second-order contribution to the phase shift, corresponding to the $(1-\mathcal{V})^{-3/2}$ term in (A3), could possibly lead to a divergence problem at the lower bound of the integral. However, it can easily be seen that the two terms of the right-hand side of Eq. (A3) vanish when ρ tends to ρ_0.

Collecting all the second-order terms [including the second-order contribution to $\Delta\rho_0$ contained in Eq. (A2)], one finally obtains the second-order contribution to the modification of the phase shift as

$$\Delta\delta^{(2)}=-\tfrac{1}{8}\int_{\rho_0}^{\infty}d\rho\,G(\rho) , \tag{A5}$$

where we have introduced

$$G(\rho)=\frac{[\Delta\mathcal{V}-(\Delta\mathcal{V}_0/\mathcal{V}_0')\mathcal{V}']^2}{(1-\mathcal{V})^{3/2}}+2\frac{\Delta\mathcal{V}_0}{\mathcal{V}_0'}\frac{(\Delta\mathcal{V}_0/\mathcal{V}_0')\mathcal{V}''-2\Delta\mathcal{V}'}{(1-\mathcal{V})^{1/2}} . \tag{A6}$$

[1]N. K. Glendenning, *Direct Nuclear Reactions* (Academic, New York, 1983).

[2]G. R. Satchler, *Direct Nuclear Reactions* (Clarendon, Oxford, 1983).

[3]W. E. Frahn, *Diffractive Processes in Nuclear Physics* (Clarendon, Oxford, 1985).

[4]C. E. Thorn, M. J. Le Vine, J. J. Kolata, C. Flaum, P. D. Bond, and J. C. Sens, Phys. Rev. Lett. **38**, 384 (1977).

[5]W. G. Love, T. Terasawa, and G. R. Satchler, Nucl. Phys. **A291**, 183 (1977).
[6]A. J. Baltz, S. K. Kauffmann, N. K. Glendenning, and K. Pruess, Nucl. Phys. **A327**, 221 (1979).
[7]P. Fröbrich, R. Lipperheide, and H. Fiedeldey, Phys. Rev. Lett. **43**, 1147 (1979).
[8]M. A. Nagarajan, A. B. Balantekin, and N. Takigawa, Phys. Rev. C **34**, 894 (1986), and references therein.
[9]N. Takigawa, F. Michel, A. B. Balantekin, and G. Reidemeister, Proceedings of the Workshop on Heavy Ion Collisions at Energies Near the Coulomb Barrier, Daresbury, England, 1990 [Inst. Phys. Conf. Ser. **110**: Section 2, 205 (1991)].
[10]H. Esbensen, S. Landowne, and C. Price, Phys. Rev. C **36**, 2359 (1987).
[11]R. Lipperheide, H. Massmann, and H. Rossner, Nucl. Phys. **A366**, 119 (1981); R. Lipperheide, H. Rossner, and H. Massmann, *ibid.* **A394**, 312 (1983).
[12]M. Abramowitz and I. A. Stegun, *Handbook of Mathematical Functions* (Dover, New York, 1972), p. 887.
[13]D. M. Brink, *Semi-classical Methods for Nucleus-Nucleus Scattering* (Cambridge University, Cambridge, 1985).